Non-markovian dynamics of double quantum dot charge qubit with static bias

Xiufeng Cao*, Hang Zheng

Department of Physics, Shanghai Jiaotong University,

Shanghai 200240, People's Republic of China

Abstract

The dynamics of charge qubit in double quantum dot coupled to phonons is investigated theoretically. The static bias is considered. By means of the perturbation approach based on unitary transformations, the dynamical tunneling current is obtained explicitly. The biased system displays broken symmetry and a significantly larger coherence-incoherence transition critical point α_c. We also analyzed the decoherence induced by piezoelectric coupling phonons in detail. The results show that reducing the coupling between system and bath make coherence frequency increase and coherence time prolong. To maintain quantum coherence, applying static bias also is a good means.

Key word: static bias, charge qubit, phonon

PACS numbers: 73.23.Hk, 73.63.Kv, 03.65.Yz, 03.67.Lx

---

* Email: cxf@sjtu.edu.cn

1. Introduction

Since the discovery that quantum algorithms can solve certain computational problems much more efficiently than classical ones[1], attention has been devoted to the physical implementation of quantum computation. Nanofabrication technology now allow us to design artificial atoms (quantum dots) and molecules (coupled quantum dots), in which atomic (molecular) -like electronic states can be controlled with external gate voltages[2, 3, 4]. As the system always interacts with its environment, quantum decoherence in the system usually is the most serious obstacle to produce efficient quantum circuits[5, 6, 7]. For the reason, a detailed understanding of quantum decoherence in open system and implementing sufficiently high number of coherent manipulation within the characteristic coherence time of qubits are crucial for future actual implementation of quantum nanostructures to quantum information technology.

To build a quantum computer, the first step is the realization of the basic device units for quantum information processing called quantum bit (qubit). Within the last decade, various schemes have been proposed and many of them have even been realized, such as superconducting flux qubit[8, 9, 10, 11] and solid charge qubit[3, 4, 12], including single and double dot qubit. Among them, the gate voltage controlled semiconductor charge qubit has the potential advantages of being arbitrarily scalable to large system and compatible with the current microelectronics technology. Recently, Hayashi et al.[13] have successfully realized coherent manipulation of electronic state in double-dot system implemented in a GaAs/AlGaAs heterostructure containing a two dimensional electron gas. The damped oscillation of population inversion is observed in the time domain and the dependent of decoherence rate T_2^{-1} on the energy offset ε is presented. In another similar experiment[14], the base material used of the charge qubit is an industry-standard silicon-on-insulator wafer with aphosphorous-doped active region and all operations (initialization, manipulation, and measurement) are achieved by capacitively coupled elements. The change in gate voltage V_{g3} can principally control static bias ε. From above, we can see it is necessary to investigate the effect of the static bias on the tunneling current of the charge qubit.

In this work, we study coherence dynamics of double QDs charge qubit using spin boson model with static bias, which is investigated without applying the Markov approximation to the electron-phonon interaction. A simple explicit expression of population inversion or tunneling current is presented through perturbation treatment based on unitary trans-

formations. The coherence-incoherence transition critical point α_c versus bias is gained. Furthermore, the piezoelectric potential phonons induced decoherence are investigated in detail and possible means for maintaining quantum coherence are expressed.

The paper is organized as follows: in Sec. 2 we introduce the model Hamiltonian for static bias spin-boson model and solve it in terms of a perturbation treatment based on unitary transformations. We analyze the result and provide proposition for how to maintain tunneling current in Sec. 3. Finally, the conclusion is given in Sec. 4.

2. The model and theory

The model we study is the spin-boson Hamiltonian for static bias[15] where the two state system is linearly coupled to a continuum of harmonic oscillators, i.e:

$$H = H_s + H_b + H_i \tag{1}$$

where H_s is the Hamiltonian of the system, H_b of the bath and H_i of their interaction that is responsible for decoherence. Here

$$H_s = -\frac{\Delta \sigma_x}{2} + \frac{\varepsilon \sigma_z}{2} \tag{2}$$

$$H_b = \sum_k \omega_k b_k^+ b_k \tag{3}$$

$$H_i = \frac{1}{2} \sum_k g_k (b_k^+ + b_k) \sigma_z \tag{4}$$

with σ_i being pauli spin matrices. Δ describes the tunneling coupling between the two states while ε is the energy offset between the uncoupled charge states. $b_k^+(b_k)$ and ω_k are the creation (annihilation) operator and energy of the phonons with the wave vector k. g_k describe the electron-phonon coupling strength. In this work we consider the static bias case with temperature T=0. The effect of the phonon bath are fully described by a spectral density:

$$J(\omega) = \sum_k g_k^2 \delta(\omega - \omega_k). \tag{5}$$

In order that the Hamiltonian is diagonalized in σ_z direction, we make a displacement to all boson modes,

$$b_k = a_k - \frac{g_k}{2\omega_k} \sigma_0 \tag{6}$$

where σ_0 is a constant and will be determined later. Then we apply a canonical transformation, $H' = \exp(s)H\exp(-s)$ with the generator[16, 17]

$$S = \sum_k \frac{g_k}{2\omega_k}(b_k^+ - b_k)(\sigma_z - \sigma_0). \tag{7}$$

Here we introduce in S a k-dependent function ξ_k. The aim of the transformation is to take into the correlation between the two states and the bath. Thus we get the Hamiltonian H' and decompose it into

$$H' = H_0' + H_1' + H_2' \tag{8}$$

where

$$H_0' = -\frac{1}{2}\eta\Delta\sigma_x + \frac{\varepsilon'\sigma_z}{2} + \sum_k \omega_k b_k^+ b_k - \sum_k \frac{g_k^2}{4\omega_k}\xi_k(2-\xi_k) + \sum_k \frac{g_k^2}{4\omega_k}\sigma_0^2(1-\xi_k)^2 \tag{9}$$

$$H_1' = \frac{1}{2}\sum_k g_k(1-\xi_k)(b_k^+ + b_k)(\sigma_z - \sigma_0) - i\frac{\eta\Delta}{2}\sigma_y \sum_k \frac{g_k}{\omega_k}\xi_k(b_k^+ - b_k) \tag{10}$$

$$H_2' = -\frac{\Delta\sigma_x}{2}(\cosh(\sum_k \frac{g_k}{\omega_k}\xi_k(b_k^+ - b_k) - \eta)$$
$$-i\frac{\Delta\sigma_y}{2}(\sinh(\sum_k \frac{g_k}{\omega_k}\xi_k(b_k^+ - b_k)) - \eta\sum_k \frac{g_k}{\omega_k}\xi_k(b_k^+ - b_k)) \tag{11}$$

with

$$\eta = \exp(-\sum_k \frac{g_k^2}{2\omega_k^2}\xi_k^2) \tag{12}$$

and

$$\varepsilon' = \varepsilon - \tau\sigma_0, \tau = \sum_k \frac{g_k^2}{\omega_k}(1-\xi_k)^2 \tag{13}$$

Obviously, H_0' can be solved exactly because in which the spin and bosons are decoupled. Then we can diagonalized H_0' by a unitary matrix U,

$$U = \begin{pmatrix} u & v \\ v & -u \end{pmatrix}, \tag{14}$$

3

with

$$u = \frac{1}{\sqrt{2}}(1 - \sin\theta)^{\frac{1}{2}}, v = \frac{1}{\sqrt{2}}(1 + \sin\theta)^{\frac{1}{2}} \tag{15}$$

and $\sin\theta = \varepsilon'/W$ with $W = (\varepsilon'^2 + \eta^2\Delta^2)^{1/2}$.

H' is transformed as follows (to the second order of g_k):

$$H'' = U^+ H' U = H_0'' + H_1'' + H_2'' \tag{16}$$

$$H_0'' = -\frac{1}{2}W\sigma_z + \sum_k \omega_k b_k^+ b_k - \sum_k \frac{g_k^2}{4\omega_k}\xi_k(2 - \xi_k) + \sum_k \frac{g_k^2}{4\omega_k}\sigma_0^2(1 - \xi_k)^2 \tag{17}$$

$$\begin{aligned} H_1'' &= -\frac{1}{2}\sum_k g_k(1 - \xi_k)(b_k^+ + b_k)(\frac{\varepsilon}{W}\sigma_z + \sigma_0) \\ &+ \frac{\eta\Delta}{2W}\sigma_x \sum_k g_k(1 - \xi_k)(b_k^+ + b_k) + i\frac{\eta\Delta}{2}\sigma_y \sum_k \frac{g_k}{\omega_k}\xi_k(b_k^+ - b_k) \end{aligned} \tag{18}$$

H_1'' and H_2'' are treated as perturbation and they should be as small as possible. For this purpose σ_0 and ξ_k are determined in such a way

$$\sigma_0 = -\frac{\varepsilon}{W}; \xi_k = \frac{\omega_k}{\omega_k + W} \tag{19}$$

that

$$H_1'' = \frac{\eta\Delta}{2}\sum_k \frac{g_k\xi_k}{\omega_k}\left[b_k^+(\sigma_x + i\sigma_y) + b_k(\sigma_x - i\sigma_y)\right] \tag{20}$$

and $H_1''|g\rangle = 0$. This is the key point in our approach. We should remark that

$$\varepsilon' = \varepsilon(1 + \frac{\tau}{W}); \sin\theta = \frac{\varepsilon(1 + \frac{\tau}{W})}{W}. \tag{21}$$

So θ is in the range of $0 \leq \theta \leq \pi/2$ and the sign of $\sin\theta$ is identical with static bias. If $\theta = 0$, the model correspond to zero bias case.

We denote the ground state of H_0'' as $|g\rangle = |s_1\rangle|\{0_k\}\rangle$, and the lowest excited states as $|s_2\rangle|\{0_k\}\rangle$, $|s_1\rangle|\{1_k\}\rangle$ where $|s_1\rangle$, $|s_2\rangle$ are eigenstates of σ_z ($\sigma_z|s_1\rangle = |s_1\rangle$, $\sigma_z|s_2\rangle = -|s_2\rangle$), $|\{n_k\}\rangle$ means that there are n_k phonons for mode k. Thus, we can diagonalize H'' as:

$$H'' = -\frac{1}{2}W|g\rangle\langle g| + \sum_E E|E\rangle\langle E| + \text{terms with higher excited states} \tag{22}$$

4

the experiments in Ref.13,14 are performed at lattice temperature below or about 20 mK. At such a low temperature, the multiphoton process is weak enough to be negligible. So we can diagonalize through the following transformation[16]

$$|s_2\rangle|\{0_k\}\rangle = \sum_E x(E)|E\rangle \tag{23}$$

$$|s_1\rangle|\{1_k\}\rangle = \sum_E y_k(E)|E\rangle \tag{24}$$

$$|E\rangle = x(E)|s_2\rangle|\{0_k\}\rangle + \sum_k y_k(E)|s_1\rangle|\{1_k\}\rangle \tag{25}$$

where

$$x(E) = (1 + \sum_k \frac{V_k^2}{(E + \frac{1}{2}W - \omega_k)^2})^{\frac{1}{2}} \tag{26}$$

$$y_k(E) = \frac{V_k}{E + \frac{1}{2}W - \omega_k} x(E) \tag{27}$$

with $V_k = \eta \Delta g_k \xi_k / \omega_k$. E are the diagnalized excitation energy and they are solutions of the equation

$$E - \frac{1}{2}W - \sum_k \frac{V_k^2}{E + \frac{1}{2}W - \omega_k} = 0 \tag{28}$$

So Hamiltonian can approximately be describes as:

$$H'' = -\frac{1}{2}W|g\rangle\langle g| + \sum_E E|E\rangle\langle E| \tag{29}$$

The population inversion can be defined as $p(t) = \langle\psi(t)|\sigma_z|\psi(t)\rangle$, where $|\psi(t)\rangle$ is the total wave function in the Schrodinger picture. Since the initialization of the charge qubit is used to in the state $|L\rangle$, it is reasonable to choose initial state $|\psi(0)\rangle = e^{-s}|L\rangle|0_k\rangle$. Then we can obtain

$$p(t) = \left\langle\psi(0)\left|Ue^{iH''t}U^+e^sUU^+\sigma_zUU^+e^sUe^{-iH''t}U^+\right|\psi(0)\right\rangle \tag{30}$$

$$= -u^2\sin\theta - v^2\sin\theta \sum_{kk'EE'} y_{k'}^*(E')y_k(E)x(E)x^*(E)e^{i(E-E')t}$$

$$-v^2\sin\theta \sum_{EE'} |x(E)|^2\left|x(E')\right|^2 e^{i(E-E')t}$$

$$+uv\cos\theta \sum_E (|x(E)|^2 e^{i(E+\frac{w}{2})t} + |x(E)|^2 e^{-i(E+\frac{w}{2})t}) \tag{31}$$

For the different terms appearing in Eq.(31), we employ the orthogonal property

$$\sum_k y_k(E)y_k(E') = \delta(E - E') - x(E)x(E') \tag{32}$$

and the residue theorem

$$\sum_E \mid x(E) \mid^2 e^{iEt} \tag{33}$$

$$= e^{-i\frac{W}{2}t} \frac{1}{2\pi i} \int \frac{e^{i(E+\frac{W}{2})t}dE}{(E - \frac{1}{2}W - \sum_k \frac{V_k^2}{E+\frac{1}{2}W-\omega_k})} \tag{34}$$

$$= e^{-i\frac{W}{2}t} \frac{1}{2\pi i} \int \frac{e^{iE't}dE'}{(E' - W - \sum_k \frac{V_k^2}{E'-\omega_k})} \tag{35}$$

Denoting the real and imaginary part of $\sum_k \frac{V_k^2}{\omega-\omega_k\pm i0^+}$ as R(ω) and $\mp\gamma(\omega)$, respectively, we can get

$$R(\omega) = \wp \sum_k \frac{V_k^2}{\omega - \omega_k} \tag{36}$$

$$= (\eta\Delta)^2 \wp \int_0^\infty d\omega' \frac{J(\omega')}{(\omega - \omega')(\omega' + \eta\Delta)^2} \tag{37}$$

$$\gamma(\omega) = \pi \sum_k V_k^2 \delta(\omega - \omega_k) = \pi(\eta\Delta)^2 \frac{J(\omega)}{(\omega + \eta\Delta)^2} \tag{38}$$

where $\wp$ stands for Cauchy principal value, and $J(\omega)$ is the spectral density.

The contour integral in Eq.(35) can be proceed by calculating the residue of integrand and substituting in Eq.(31), we obtain

$$p(t) = -\sin\theta + \sin\theta(1 + \sin\theta)e^{-2\gamma(\omega)t} + \cos^2\theta\cos(\omega_0 t)e^{-\gamma(\omega)t} \tag{39}$$

where ω_0 is the solution to the equation

$$\omega - W - R(\omega) = 0 \tag{40}$$

Thus a rather simple expression for the dynamical tunneling is obtained analytically. It should be noted here that for t→ ∞, our result tend towards thermodynamics equilibrium value[18], which is modulated by static bias

$$p(\infty) = -\sin\theta = -\frac{\varepsilon(1 + \frac{\tau}{W})}{W} \tag{41}$$

6

Comparing with Markovian approximation, our result not only give the long time limit behavior, but the short time damping coherence oscillation. That must holds most prominently if semiconductor quantum dots are to be used as basic building blocks for quantum information processing where the operation completely relies on the presence of coherence.

Finally, the tunneling electron population in the right dot at time t can be obtain $n(t) = \frac{1+\langle \sigma_z(t) \rangle}{2} = \frac{1+p(t)}{2}$.

Until here, our presentation is not restricted by the form of the spectral density and can be extended to all kinds of baths. Previous work states that, at zero temperature in double-dot system of GaAs material, the dominant contribution of phonons to QDs come from the piezoelectric coupling and the deformation potential coupling is small enough to be ignored. So we will use the piezoelectric coupling spectral density[17, 19]:

$$J(\omega) = \alpha\omega(1 - \frac{\omega_d}{\omega}\sin\frac{\omega}{\omega_d})\theta(\omega_c - \omega) \tag{42}$$

where α is the dimensionless coupling constant, $\omega_c = s/l$ and $\omega_d = s/d$ (s is the sound velocity in crystal, l is the dot size and d is the center-to-center distance between two dots) and $\theta(x)$ is the usual step function.

3. The result and discussion

From Eq.(39) we have been able to obtain the population inversion of charge qubit $p(t)$ as the analytical damped oscillation form with frequency ω_0 and damping rate $\gamma(\omega)$. In the following calculations, ω_c is taken as the energy unit. We choose the quantum dot size l as 100nm (approximate size for the dot in Ref.13), i.e. $\omega_c = 32.5$ μeV (or 0.05 ps^{-1}). Assume the distance between two dots is sufficiently large, d=667 nm, correspondingly $\omega_d = 0.15\omega_c$. The typical value of tunneling barriers in experiment[13] are $\Delta = 9$ μeV. Without special indication, Δ is choosen 9 μeV.

First we illustrate the population inversion as function of time ($\omega_c t$) in fig.1(a) with five different static bias: $\varepsilon = -8$ μeV (dashed line), 0μeV(solid line), 8μeV (dotted line) for fixed $\alpha = 0.04$. It is clearly shown that the population inversion exhibit damping oscillation and symmetry broken. The asymptotic value of t he long time limit $p(\infty)$ is determined by the static bias. If bias is zero, $p(\infty) = 0$.

Fig.1(b) presents the long time limit of population inversion or the thermodynamics equilibrium value $p(\infty) = -\varepsilon'/W$ as functions of bias ε. Comparing with the results of NIBA[18], which is expressed as $p(\infty) = -\varepsilon/\sqrt{\varepsilon^2 + \Delta_r^2}$, on the scale of the figures, the two

curves are overlapped if the identical Ohmic spectral density $J(\omega) = 2\alpha\omega\theta(\omega_c - \omega)$ is used. While the system is in the piezoelectric potential bath, $p(\infty)$ deviate a little.

Fig.1(c) sketches the coherence-incoherence critical point α_c versus ε/ω_c for fixed $\Delta = 9$ μeV in Ohmic bath. We see that bias increases α_c significantly and induce a transition from strongly damped incoherent to coherent oscillation behavior. The similar result is also obtained by Klaus[15] from Monte Carlo simulations.

The quantum coherence depends on two factors: oscillation frequency ω_0 and decoherence rate T_2^{-1}. It is already noticed that long coherence time is favorable for quantum manipulation. However low oscillation frequency means that the number of quantum operation that can be achieved within the coherence time is very limit[14]. So we must give attention to two aspects coherence time and oscillation frequency. In what follows, we analyse the effect of the static bias ε, the tunneling energy Δ and e-p coupling constant α on the decoherence rate γ and the damping oscillation frequency ω and elucidate the advantage and disadvantage for changing characteristic energy Δ and ε or decreasing e-p coupling to remain quantum coherence.

In contrast with experiment, we present the decoherence rate γ (T_2^{-1}) as function of energy offset ε[Fig. 2]. The electron-phonon coupling constant $\alpha = 0.02 - 0.07$ is used to explain the inelastic current in GaAs/AlGaAs heterostructure DQD samples[19]. In Fig.2(a) we shows the damping rate γ as a function of static bias ε with three different e-p coupling $\alpha = 0.04$ (solid), $\alpha = 0.08$ (dashed) $\alpha = 0.12$ (dotted). These curves show clearly that the decoherence rate raise with increasing of the absolute value of the bias ε. The vary of γ vs ε is agree with the result of experiment. If $\varepsilon = 0$ μeV and $\alpha = 0.04$, decoherence rate γ approximately is 0.2 ns^{-1}. Increasing the e-p coupling to $\alpha = 0.12$ the damping rate contributing from piezoelectric phonons grow up to 0.50 ns^{-1}, occupy more than half of the experimental result. It proves that the coupling to the piezoelectric potential phonons is one of the main decoherence mechanisms in such a double-dot system.

The damping oscillation frequency ω_0 vs bias ε is shows in Fig.2(b), and the parameters are same as those in Fig.2(a). The qubit oscillation frequency can be changed continually by bias voltage and behave nonlinear response versus ε, which explain the experimental result in Ref.14. Setting large static bias can efficiently improve oscillation frequency. When $\alpha = 0.04$ and $\varepsilon = 0$ μeV, the frequency approximately is 2.1 GHz, which is extraordinarily agree with the fit result of the experimental data in Ref.15. The decoherence rate and the

oscillation frequency reveal symmetry about bias.

Fig.3(a) presents the decoherence rate as function of tunneling coupling Δ at three different static bias $\varepsilon = 0$ μeV (solid), 3 μeV (dashed), 6 μeV (dotted), fixing α as 0.04. Enlarging tunneling coupling Δ between two dots make damping rate γ gradually increase as shown in Fig.3(a). So quantum coherence can be remained by reducing tunneling barrier. In experiment, the barrier tunneling can be principally defined by the materials and the geometrical constriction between the dots in the fabrication of the device. But it is possible to modify the tunneling barrier by gate voltages, just as shown in Ref.13 Fig.2(d). From Fig.3(a), if Δ in the order of magnitude of μeV, the decoherence rate is probably in the range of $0.2 \sim 1$ ns^{-1}, which is agree well with the Ref.13. A plot of oscillation frequency ω as function Δ is shown in Fig.3(b). At zero bias $\varepsilon = 0$, the curve behavior is approximately line. Increasing static bias, ω appear nonlinear response. Comparing two similar experiment in Ref.15 and Ref.16, the characterized energies E^* 40.5 neV corresponding to angular frequency $\omega = 62$ MHz in the silicon two-level quantum system are 1/37 smaller than quantum level spacing 1.5 μeV corresponding to oscillation frequency $\omega = 2.3$ GHz in the reports for semiconductor double quantum dot charge qubit. From the calculation result, we can deviate that the reducing of energy split make damping rate and oscillation frequency fall same order of magnitude, correspondingly, in the piezoelectric coupling spectral density, so the lack of piezoelectric coupling in the silicon QD might result in the long coherence time two orders of magnitude longer than reports for semiconductor QD. We find that the bias can effectively enhance oscillation frequency but have relative little lifting for damping rate in the case of weak tunneling couple. Therefore adjust static bias larger is another choice to preserve coherence and that is a suggestion to overcome the obstacle in Ref.16.

Fig.4 presents the decoherence rates γ and oscillation frequency ω as functions of dimensionless coupling constant α at three different bias $\varepsilon = 0$ μeV (solid), 3 μeV (dashed), 6 μeV (dotted). As shown in Fig.4(a), for determined bias, it is an almost linear relation between damping rate γ and dimensionless coupling constant α. Fig.4(b) displays the oscillation frequency ω versus coupling constat α. These curves show clearly that when the coupling constant α become weaker three or two orders of magnitude from 0.04, the oscillation frequency ω have linearly increased, albeit very relaxedly. Applied static bias, the decoherence rate and oscillation frequency always are enhanced. As a result, to keep the coherence of charge qubit in long time, one good way is to minish the coupling with environment, either

by find good material with small e-p coupling, or by modifying the design of the DQD structure, or by better gate tuning.

Anyway, to realize quantum computation, the important direction are to reduce the coupling to environment by all means, but to ensure effective interdot coupling and static bias.

4. Conclusion

We studied the charge qubit dynamics with static bias by a perturbation treatment based on two times unitary transformations. Our approach applies to all forms of spectral density. In Ohmic bath, the result shows that α_c clearly increases and population inversion breaks symmetry in biased system. Analyzing the piezoelectric coupling phonon induced decoherence, we find that, weak coupling of the charge qubit to the environment carries out large coherence oscillation frequency and long coherence time. When tunneling coupling between two QDs is fixed, adjust gate voltage to enlarge static bias make oscillation frequency observably increase while damping rate unnoticeably increase. That is another better choice to maintain quantum coherence. Finally we hope that our predictions can offer advice for experimenter and be testified by experiment in the near future.

————————

[1] M. A. Nielsen and I. L. Chuang, *Quantum computation and quantum information* (Cambridge University Press, United Kingdom, 2000).

[2] S. Tarucha, D. G. Austing and T. Honda, Phys. Rev. Lett. **77**, 3613 (1998).

[3] T. H. Oosterkamp *et al.*, Nature **395,** 873 (1998).

[4] Toshimasa Fujisawa, Tjerk. H. Oosterkamp *et al.*, Science **282**, 932 (2001).

[5] V. N. Stavrou and Xuedong Hu, Phys. Rev. B **72**, 075362 (1999).

[6] W. G. Unruh, Phys. Rev. A **51**, 992 (1995).

[7] S. D. Barrett, G. J. Milburn, Phys. Rev. B **68**, 155307 (2003).

[8] P. Bertet, I. Chiorescu, G. Burkard *et al.*, Phys. Rev. Lett. **95**, 257002 (2005).

[9] I. Chiorescu, P. Bertet, K. Semba *et al.*, Nature **431,** 159 (2004).

[10] I. Chiorescu, Y. Nakamura, C. J. P. M. Harmans and J. E. Mooij, Science **299**, 1869 (2003).

[11] A. Lupascu, E. F. C. Driessen. L. Roschier *et al.*, Phys. Rev. Lett. **96**, 127003 (2006).

[12] S. Gardelis, C. G. Smith and J. Cooper *et al.*, Phys. Rev. B **67**, 073302 (2003).

[13] T. Hayashi et al, Phys. Rev. Lett. **91**, 226804 (2003).

[14] J. Gorman, D. G. Hasko and D. A. Williams, Phys. Rev. Lett. **95**, 090502 (2005).

[15] Klaus Volker, Phys. Rev. B **58**, 1862 (1998).

[16] H. Zheng, Eur. Phys. J. B **38**, 559 (2004).

[17] Zhuo-Jie Wu, Ka-Di Zhu *et al.*, Phys. Rev. B **71**, 205323 (2005).

[18] U. Weiss, *Quantum dissipative system*, (World Scientific, Singapore, 1993).

[19] T. Brandes and T. Vorranth, Phys. Rev. B **66**, 075341 (2002).

FIGURES

Fig.1.(a) The population difference as a function of $\omega_c t$ for different static bias $-8\ \mu eV$ (dashed line), $0\ \mu eV$ (solid line), $8\ \mu eV$ (dotted line). (b) The long time limit $p(\infty)$ (solid) as a function of static bias ε in piezoelectric potential bath. $p(\infty)$ (dotted) in Ohmic bath and $p(\infty)$ (dashed) in Ohmic bath for NIBA. The coupling constant is fixed as $\alpha = 0.04$. (c) The coherence-incoherence critical point α_c versus static bias ε/ω_c with $\Delta = 9\ \mu eV$.

Fig.2. The damping rate γ and oscillation frequency ω versus ε in (a) and (b), respectively with $\Delta = 9\ \mu eV$, $\omega_d = 0.15\omega_c$ for different $\alpha = 0.04$ (solid line), 0.08 (dashed line), 0.12 (dotted line).

Fig.3 The damping rate γ and oscillation frequency ω versus Δ in (a) and (b), respectively with $\alpha = 0.04$, $\omega_d = 0.15\omega_c$ for different static bias $\varepsilon = 0\ \mu eV$ (solid line), $3\ \mu eV$ (dashed line), $6\ \mu eV$ (dotted line).
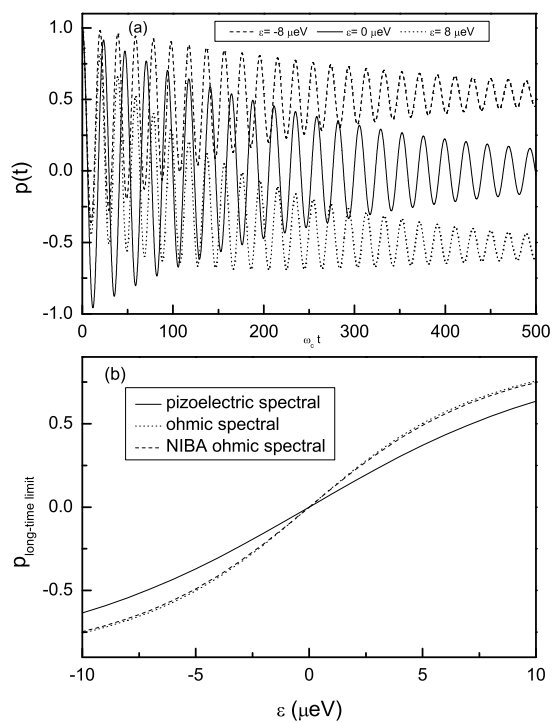
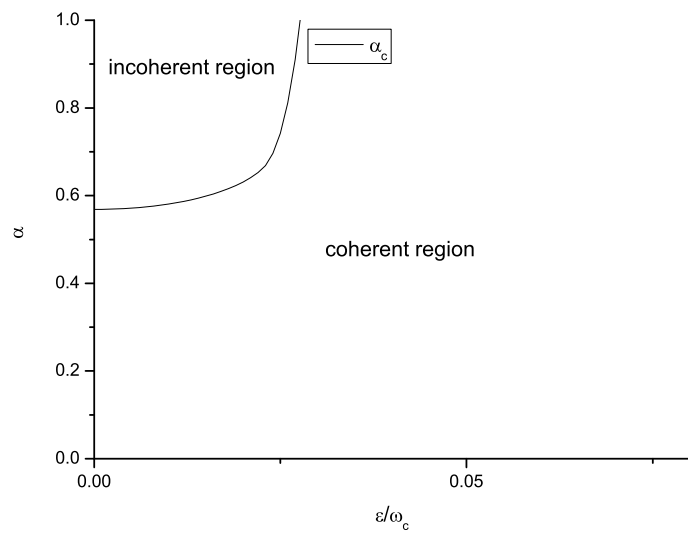Fig.4. The damping rate γ and oscillation frequency ω versus α in (a) and (b), respectively with $\Delta = 9\ \mu eV$, $\omega_d = 0.15\omega_c$ for different static bias $\varepsilon = 0\ \mu eV$ (solid line), $3\ \mu eV$ (dashed line), $6\ \mu eV$ (dotted line).
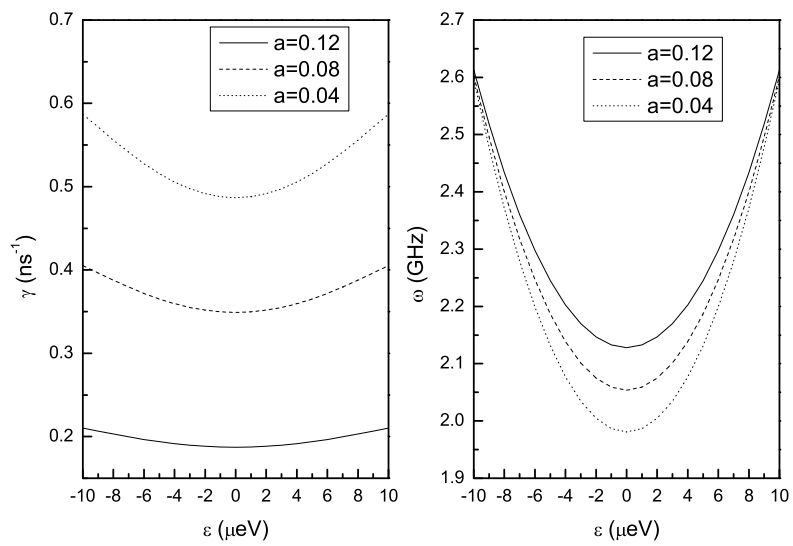
Fig.1

(a) ε= -8 μeV   ε= 0 μeV   ε= 8 μeV

(b) pizoelectric spectral
ohmic spectral
NIBA ohmic spectral

Fig1.c

Fig.2

Fig.3

Fig.4